Efficient electron open boundaries for simulating electrochemical cells

Mario G. Zauchner* and Andrew P. Horsfield†
Department of Materials and Thomas Young Centre,
Imperial College London, South Kensington Campus, London SW7 2AZ, U.K.

Tchavdar N. Todorov‡
Atomistic Simulation Centre, School of Mathematics and Physics,
Queen's University Belfast, Belfast BT7 1NN, U.K.
(Dated: January 3, 2018)

Non-equilibrium electrochemistry raises new challenges for atomistic simulation: we need to perform molecular dynamics for the nuclear degrees of freedom with an explicit description of the electrons, which in turn must be free to enter and leave the computational cell. Here we present a limiting form for electron open boundaries that we expect to apply when the magnitude of the electric current is determined by the drift and diffusion of ions in solution, and which is sufficiently computationally efficient to be used with molecular dynamics. We present tight binding simulations of a parallel plate capacitor with nothing, a dimer, or an atomic wire situated in the space between the plates. These simulations demonstrate that the new scheme can be used to perform molecular dynamics simulations when there is an applied bias between two metal plates with at most weak electronic coupling between them. This simple system captures some of the essential features of an electrochemical cell, suggesting this approach might be suitable for simulations of electrochemical cells out of equilibrium.

I. INTRODUCTION

A traditional electrochemical experiment involves at least two electrodes immersed in an aqueous solution[1], with the reactions that take place depending on the bias applied between those electrodes. This arrangement can apply to batteries, electrolysis, and even corrosion. Two key features of this system are: electrons can flow onto and off the electrodes; the reactions occur when the system is out of equilibrium. To simulate this system we need to capture these two features.

An appropriate simulation methodology thus must be able to combine open boundary conditions for the electrons with molecular dynamics (MD) for the solution. This puts very tight efficiency constraints on the open boundary formalism as even MD performed with ground state electronic structure methods can be computationally very demanding. Here we present an open boundary formalism appropriate for electrochemical problems that has essentially the same computational cost as ground state electronic structure methods.

We note that important insights have been arrived at by means of equilibrium simulations which can address aspects of the problem. For example, the variation of interface properties with electron chemical potential can be investigated by adding electrons to the computational cell[2], and dynamic simulations to determine the symmetry factor associated with the detachment of an ion have been performed[3].

While there are several well tested codes for open boundaries[4–7], these tend to be computationally too expensive for non-equilibrium MD. The Hairy Probes (HP) method[8,9] has previously been shown to be an efficient solution for electron open boundary simulations of nanoscale systems. However, even the standard HP method is not efficient enough for MD over larger time scales. Fortunately, for the specific case of electrochemistry we can exploit the fact that the current is carried by ions in solution, rather than ballistic electrons, to produce a simplified version of HP. It was speculated in an earlier paper that this might be a possible approach[8]; here we illustrate how the method works in practice.

The key point is that the time scale for electron transport from one electrode to another is set by the rate at which ions diffuse, which is much longer than that for ballistic transport of electrons over the same distance. This allows us to impose the condition that electrons enter and leave the computational cell slowly without restricting the net current flow. Mathematically, this translates to weak coupling of the external leads that connect the system to electron reservoirs, which in turn permits drastic simplification of the open boundary equations. The choice of electrochemical potential and temperature of the reservoirs corresponds to the potentials and temperatures of the electrodes, with which the reservoirs are assumed to be in local equilibrium.

In this limit we regain the familiar single particle picture with molecular orbitals populated by electrons[8], but the population of a given level is now controlled by the attached probes and their associated electrochemical potentials. This allows different electrochemical potentials to operate within the system, producing non-equilibrium conditions, while retaining the efficiency of traditional ground state electronic calculations. We note that this method is very straightforward to incorporate into existing electronic structure codes.

This approach is similar in spirit to earlier work by Bonnet *et al*[10]. The formalism of Bonnet *et al* employs a pseudodynamic set of equations to allow electrons from a weakly coupled reservoir (it does not modify the elec-

tronic states) to be added or removed from the system until the electrochemical potentials of the reservoir and system equilibrate. Here, we instead treat the injection of electrons using scattering theory in the long time limit, and the orbital populations are determined once the electronic structure of the system is known. An important practical difference is that with HP we can attach electron reservoirs possessing different electrochemical potentials to different parts of the system, even when those parts are coupled electronically to each other. This is possible because we can define entry and exit points for electrons, and include the way this modifies the population of a given state. This could be important for simulating complete electrochemical cells, rather than just half cells.

We have implemented the simplified HP method in the Tight Binding (TB) package PLATO[11,12] (Package for Linear-combination of Atomic Type Orbitals). We have investigated a parallel plate capacitor consisting of two Cu plates, viewing this as the simplest approximation to an electrochemical cell we could imagine. We note that at this stage we have not introduced a solution, but have only allowed weak electron transport between the plates through the introduction of an atomic wire. Our aim here is to demonstrate the ability to perform MD under conditions roughly approximating those of an electrochemical cell (two electrodes at different potentials with at most weak electron coupling between them). There is no attempt at this stage to introduce the added complexities of double layers at the electrode interfaces, the transfer of charge from the electrodes to species in the solvent, and the drift and diffusion of charged species under potential and concentration gradients. These are all critical processes, and we will study them as soon as possible; but for now we limit our ambitions to illustrating the ability to perform MD under appropriate conditions.

We use a simple Empirical Tight Binding model to study this system, and so inspect the correctness (or otherwise) of the method. We performed static relaxation calculations of the atomic coordinates of the system under an applied voltage, to show that the forces generated by the method using the expression from Ehrenfest Dynamics[8,13] are sufficiently close to the derivative of the expression used for the total energy to allow energy conserving MD simulations. We were then able to compute the bond length and charge distribution on a copper dimer between the two capacitor plates as a function of applied bias; atoms in the capacitor plate as well as the dimer were free to move. This illustrates the ability of the method to impose an electric field, and to follow the dynamics of atoms in that field. Next, we performed MD simulations in the absence of thermostats for the dimer between charged plates to illustrate the applicability to MD. For closed boundary simulations these would be constant energy. We find that in this case energy is remarkably well conserved, even with the presence of open boundaries. Finally, to demonstrate that the method continues to perform correctly when there is weak electron coupling between the plates, we perform MD with an atomic wire present that couples the two plates to one another. We find that the plates continue to possess the net charge we would expect, while lifting the constraint of requiring the electrodes to be electronically independent.

II. FORMALISM

The method used here is based on the HP formalism, described in detail in Horsfield *et al*[8]. HP is a computational method for imposing an electric current on a nanoscale system. There are several ways to think about HP. The term probe, as used here, originates with the Landauer-Buttiker picture of mesoscopic conductors[14]. Each probe can be thought of as an atomic wire that is coupled at one end to one atomic orbital in the system, and at the other end to a reservoir of electrons with a known electrochemical potential and temperature. In HP, many probes are used to create sources and sinks of electrons, and they may not be weakly coupled. From a formal viewpoint, the electrons entering or leaving the probes are described by scattering theory or non-equilibrium Green's functions, but with some important assumptions: the density of states of a probe is uniform over a wide energy range (wide band approximation), and a probe couples to just one atomic orbital. Probe p then appears as a constant imaginary contribution $-\mathrm{i}\Gamma_p/2$ to one term on the diagonal of the system Hamiltonian matrix (see Eq. 3). The coupling Γ_p can then be interpreted as corresponding to a lifetime $\tau_p = \hbar/\Gamma_p$ for an electron sitting on the orbital to which the probe is coupled: the open boundary conditions can then be seen as allowing electrons to be created and destroyed at those sites where the probes are attached.

Following the scattering theory arguments of Todorov[15] the following expression for the single particle density matrix can be derived

$$\rho_{\beta\beta'} = 2\sum_{rs} f_{rs}\chi^{(r)}_{\beta}\chi^{(s)*}_{\beta'} \tag{1}$$

where the factor of 2 is for spin degeneracy and

$$f_{rs} = \frac{1}{2\pi}\sum_{p}\Gamma_p\zeta^{(r)*}_{\beta_p}\zeta^{(s)}_{\beta_p}\int_{E_{p,c}}^{\infty}\frac{f^{(p)}(E)}{(E-\epsilon^{(r)})(E-\epsilon^{(s)*})}\mathrm{d}E \tag{2}$$

can be thought of as a generalised occupancy. Here $\zeta^{(r)}_{\beta}$ and $\chi^{(r)}_{\beta}$ are left and right eigenstates respectively given by

$$\sum_{\beta'}\left[H_{\beta\beta'} - \delta_{\beta\beta'}\sum_{p}\frac{\mathrm{i}}{2}\Gamma_p\delta_{\beta\beta_p}\right]\chi^{(r)}_{\beta'} = \epsilon^{(r)}\sum_{\beta'}S_{\beta\beta'}\chi^{(r)}_{\beta'} \tag{3}$$

$$\delta_{rs} = \sum_{\beta\beta'}\zeta^{(r)*}_{\beta}S_{\beta\beta'}\chi^{(s)}_{\beta'} \tag{4}$$

where $\epsilon^{(r)}$ is the corresponding eigenvalue. The subscript β indexes atomic orbitals, Γ_p is the coupling strength of

probe p, $f^{(p)}$ is the Fermi function with temperature and electron chemical potential for that probe, and β_p is the orbital to which the probe is attached. The quantities $H_{\beta\beta'}$ and $S_{\beta\beta'}$ are the Hamiltonian and overlap matrices respectively.

In the limit of small coupling f_{rs} becomes diagonal with:

$$f_{rr} \to \frac{1}{2\pi}\sum_p \Gamma_p |\zeta^{(r)}_{\beta_p}|^2 \int_{E_{p,c}}^{\infty} \frac{f^{(p)}(E)}{|E-\epsilon^{(r)}|^2}\mathrm{d}E \tag{5}$$

If we rewrite $\epsilon^{(r)}$ as $\varepsilon^{(r)} - i\eta^{(r)}$ we get:

$$f_{rr} \to \frac{1}{2\pi}\sum_p \Gamma_p \frac{|\zeta^{(r)}_{\beta_p}|^2}{\eta^{(r)}} \int_{E_{p,c}}^{\infty} \frac{f^{(p)}(E)\eta^{(r)}}{|E-\varepsilon^{(r)}|^2+\eta^{(r)2}}\mathrm{d}E \tag{6}$$

$$\to \sum_p \frac{1}{2\eta^{(r)}}\Gamma_p |\zeta^{(r)}_{\beta_p}|^2 f^{(p)}(\varepsilon^{(r)}) \tag{7}$$

From first order perturbation theory we have $\eta^{(r)} = \frac{1}{2}\sum_p \Gamma_p |\zeta^{(r)}_{\beta_p}|^2$. Substituting this into Eq. 7, and assuming Γ_p is independent of p, finally yields[8]:

$$f_r = f_{rr} \to \frac{\sum_p |\zeta^{(r)}_{\beta_p}|^2 f^{(p)}(\varepsilon^{(r)})}{\sum_p |\zeta^{(r)}_{\beta_p}|^2} \tag{8}$$

which can be interpreted as the weighted average of Fermi functions from each probe.

Eq. 8 works very well for strongly bonded systems, such as metallic plates. However, in electrochemistry we encounter systems where solvent molecules are only loosely connected to the electrodes, which makes it difficult for electrons to reach solution molecules. A simple solution to this problem can be achieved by making Γ_p dependent on p again, and separating the probes into the main probes p with coupling strength Γ that impose the voltage, and solution probes s with coupling strength $\alpha\Gamma$, where $\alpha \ll 1$. If the Fermi function for the solution probes is $\bar{f}(\epsilon)$, then the expression for the occupancy becomes:

$$f_r = \frac{\alpha\bar{f}(\varepsilon^{(r)})\sum_s |\zeta^{(r)}_{\beta_s}|^2 + \sum_p |\zeta^{(r)}_{\beta_p}|^2 f^{(p)}(\varepsilon^{(r)})}{\alpha\sum_s |\zeta^{(r)}_{\beta_s}|^2 + \sum_p |\zeta^{(r)}_{\beta_p}|^2} \tag{9}$$

If the main probes do not couple at all to the state r then we get $f_r = \bar{f}(\epsilon^{(r)})$, which is the result for a ground state calculation, and is independent of α. We require α to be small so that when the main probes are coupled, their contribution to the level occupancy dominates that from the solution reservoir, ensuring a bias can be applied as desired.

It is reasonable to ask: what is the physical meaning of these solution probes? As we have just shown, they only influence the results if electrons are unable to find a path from the external reservoirs to the solution molecules. Without their addition, these molecules would have no electrons, which is unphysical. In reality they would have picked up electrons by some other process at an earlier stage, and then held onto them. The electrochemical potential we apply is then that of the system with which they were in equilibrium at the time they acquired their electrons. We take this to be the reference electrochemical potential of the reservoirs about which the bias is defined, and which is set to ensure the system overall is electrically neutral. We also note that these probes enable charge redistribution between the solution molecules, which mimics electron tunneling, but without coherence.

The energy of a system is not well defined when we have open boundaries. However, in this simplified formalism we compute energy using the same expression as for ground state calculations, but with the molecular orbital populations given by Eq. 9. The forces are evaluated using the expression

$$F_\nu = -\mathrm{Tr}\left\{\rho\frac{\partial H}{\partial R_\nu}\right\} - \frac{\partial\Phi}{\partial R_\nu} \tag{10}$$

where F_ν is a component of the atomic forces (ν combines the atomic index and direction), R_ν is a component of the atomic positions, ρ is the single particle density matrix, H is the single particle Hamiltonian, and Φ combines the nuclear-nuclear interaction and double counting terms. This expression corresponds to treating the forces as originating from an Ehrenfest Dynamics calculation[13]. We note there is an additional subtlety here. For the case where all probes have the same temperature and electrochemical potential, we get back the result for a closed system, independent of the number of probes and where they are attached. In this case we would expect the forces to be the derivative of the free energy[16], for which we would need to include the entropic term in our energy, something we do not do. So there are in principle two sources of error (the missing entropy, and the presence of open boundaries). For small temperatures, the entropic term will be small. This is explored below.

III. METHOD

The limiting case of the HP method for weakly coupled probes was added to the TB software PLATO. To study the behaviour of the new algorithm, we investigated a parallel plate capacitor consisting of a total of 256 Cu atoms (128 per plate), with 64 probes attached to the outer atoms of each plate. The solution probes with coupling of $\alpha\Gamma$ are then applied to all other atoms (in this case, the two layers in the plates facing the opposite plate plus any atoms placed between the plates). We used an orthogonal tight binding model by Sutton *et al.*[17], where one s orbital is assigned to each atom. Each atom is allowed to acquire a monopole charge, with the Coulombic interaction being allowed to extend to infinity; the on-site repulsion is given by $U = 6.80$ eV. All probes have vanishingly small coupling strength and a temperature of $k_B T_p = 0.0136$ eV. The temperature enters through the

Fermi function assigned to each probe, and determines the electron population associated with the probe.

In the first step of the simulation, a single arbitrary electrochemical potential is assigned to every probe. The algorithm then adjusts this one chemical potential until the system as a whole is charge neutral. The determined chemical potential is then used as the reference chemical potential of the system.

In the next step of the simulation a bias is applied, which leads to an anti-symmetric shift in the chemical potential of the two terminals: half the bias is added as a positive shift in the electron chemical potential to the probes attached to one plate, while half is added as a negative shift to the other plate. By varying the applied bias we determined the net charge on one plate as a function of applied bias. The setup is illustrated in Fig. 1a. Note that the plates are far enough apart that there is zero electron hopping between them. To maintain global charge neutrality, we adjust the reference electrochemical potential once a bias is applied.

The process was then repeated for the system shown in Fig. 1b in which a copper dimer has been added between the plates. The bond length of the copper dimer was computed for different voltages. Note that the separation between the copper plates was doubled to ensure the dimer does not form a bond with the copper plates.

Next, the relaxed system with an applied bias of 0.408 V was used to perform a simple molecular dynamics simulation. Finally, MD was performed with an atomic wire connecting the inner surfaces of the two plates.

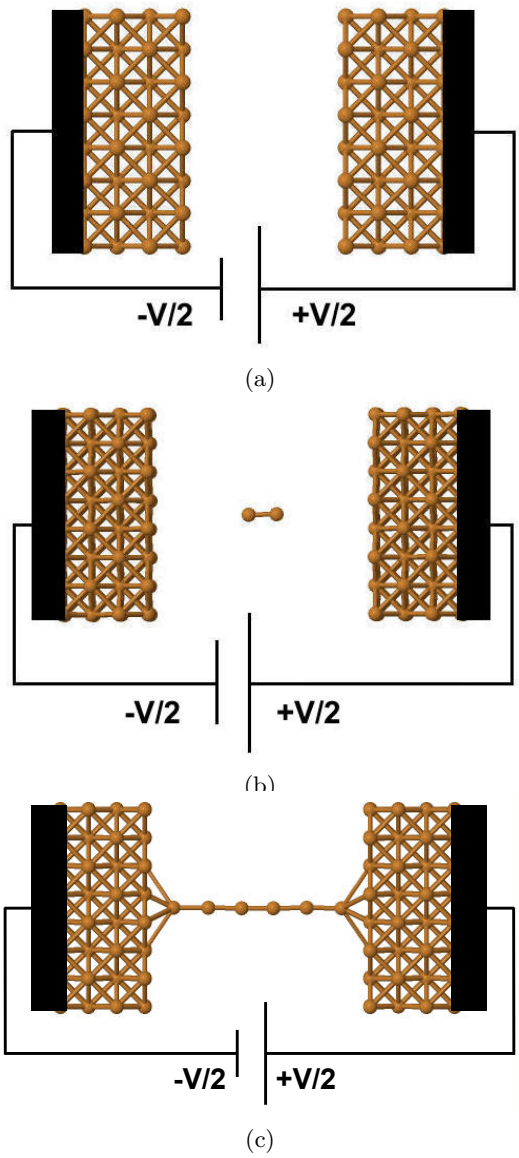

FIG. 1: Capacitor setup for the Hairy Probes calculations. There is a total of 256 Cu atoms (128 per plate), with 64 probes attached to the outer two planes of atoms on each plate. a) The setup for determination of the charge distribution, and the net charge as a function of applied voltage. b) The setup for the dimer bond length calculations. Note that the separation of the plates was doubled relative to the previous case to ensure the dimer is not connected to the plates. c) The setup for the simulations with an atomic wire between the plates.

IV. RESULTS

A. Parallel plate capacitor

For a range of values of the coupling coefficient α, we determined the total charge on one plate as a function of the applied bias. From the capacitor law $Q = CV$ (where Q is the charge on a plate, C is the capacitance, and V is the applied voltage), one would expect a linear dependence of Q on V. From the slope of the line relating charge to voltage we can determine the capacitance as a function of α. From Fig. 2 we see that there is a plateau for low coupling strengths. This occurs because the left and right chemical potentials have entered regions of low density of states. Once they re-enter regions of higher density of states the charge continues to increase with a similar slope as before. For the determination of the capacitance, we fit a straight line to the region before the plateau. The capacitance as a function of solution probe coupling is shown in Fig. 3: the difference between the two curves is explained below. The lowering of capacitance as α increases can be explained as follows. As α increases, the relative contribution of the main probes (which have a finite bias applied) is lowered, while that from the solution probes (with zero applied bias) increases, leading to a decrease in the effective applied bias experienced by the plates. Thus we need to apply a higher external bias to generate a given charge, leading to a reduced capacitance.

In Fig. 4 we show the charge distribution inside the capacitor. We see that there is a concentration of charge on the innermost and outermost planes of atoms. This suggests two definitions of the capacitance, with the two lines

in Fig. 3 corresponding to these two definitions. One is the usual definition of capacitance $C = Q/V$ where Q is the total charge on the plate, and V the applied voltage between the plates. The other definition is $C = Q_{\text{inner}}/V$ where Q_{inner} is the charge on the two planes in a plate nearest the opposite plate. This second definition is interesting as it leads to better agreement with the standard parallel plate capacitor expression $C = \epsilon_0 A/d = 0.16$ e/V where ϵ_0 is the permittivity of free space, A is the area of the capacitor plate, and d is the separation between the plates. The better agreement follows from the derivation of this standard expression: it assumes charge distributed over one face of each plate.

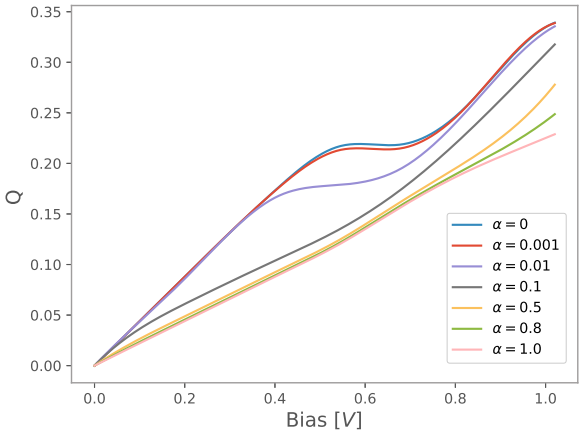

FIG. 2: The total charge accumulated on a capacitor plate for different voltages for a parallel plate capacitor. The capacitor consists of 256 Cu atoms, 128 atoms per plate. A range of values of the solution probe coupling α is considered. Note the shoulder for small values of α.

Under an applied bias of 0.816 V, we relaxed the forces on the atoms in the capacitor as shown in Fig. 1a. We find that the forces are accurate enough to lower the system's energy in a smooth fashion upon relaxation, as shown in Fig. 5. We see that the energy decreases sharply over the first 100 steps, and then remains relatively constant at the equilibrium value.

B. Bond length of copper dimer under applied bias

In the next set of simulations we relaxed the forces on a copper dimer in between the plates of the capacitor, and determined the bond length as a function of bias. We used a solution probe coupling strength α of 0.01 for all of the simulations: this is applied to the dimer and the atoms in the plates near the surfaces facing the opposite plates. In Fig. 6a we observe a quadratic dependence of the bond length with respect to the applied bias. This simulation can be thought of as a rough approximation to the inclusion of a solute or solvent molecule between the plates.

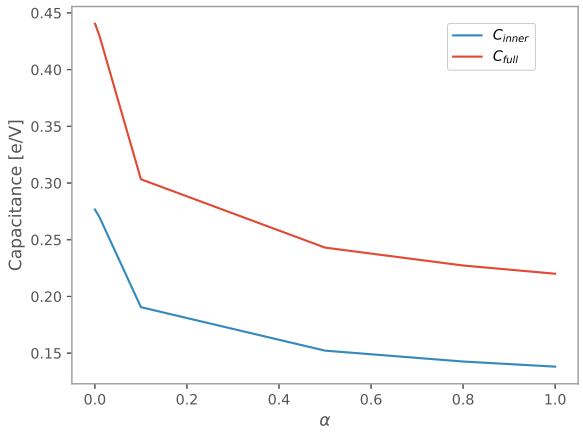

FIG. 3: Dependence of capacitance on solution probe coupling. For the red (upper) line, the capacitance is given by the total charge on a plate, divided by the applied voltage. For the blue (lower) line the capacitance is defined as the charge on the half of the plates closest to the opposite plates, divided by the applied voltage.

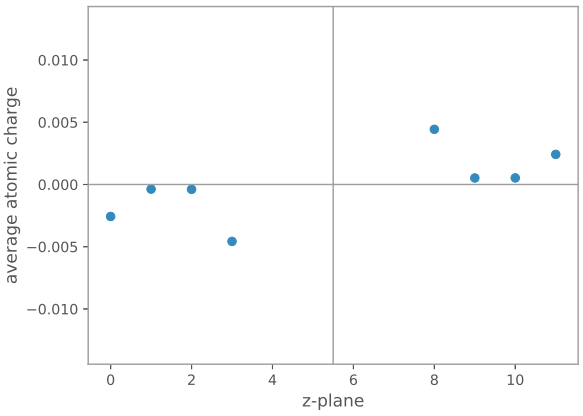

FIG. 4: Average charge per atom on each plane of atoms in the capacitor plates at 0.408 V bias and solution coupling strength $\alpha = 0.0$. Note the increased charge at the outermost and innermost layers of the plates. The x-axis is the number of the plane of atoms, starting at zero, with the vacuum treated as a series of missing planes. The mid-point between the plates lies between planes 5 and 6.

We can understand the dependence of bond length on applied bias directly from the TB model. Our symmetric dimer has one s-orbital per site with zero onsite energy, contains N electrons, a hopping matrix element $v(r) = -v_0(r_0/r)^q$ and a pair potential $\phi(r) = \phi_0(r_0/r)^p$. This

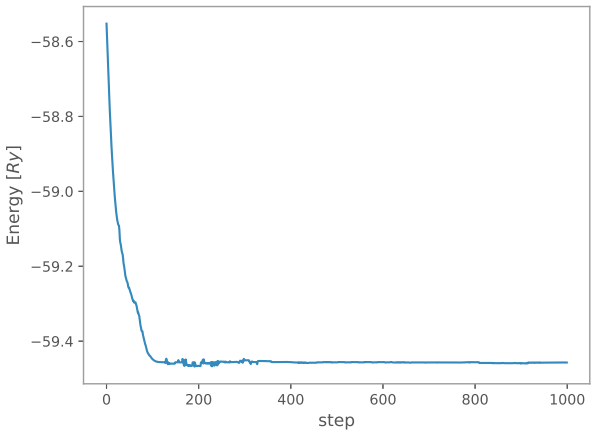

FIG. 5: Evolution of the energy of the capacitor upon relaxation under an applied bias of 0.816 V.

gives a total energy E which has the form:

$$E(N,r) = -Nv_0\left(\frac{r_0}{r}\right)^q + \phi_0\left(\frac{r_0}{r}\right)^p \tag{11}$$

Here, r_0 is a reference distance, and v_0 and ϕ_0 the values of the corresponding hopping matrix element and pair potential respectively. These values, plus the powers p and q, are taken from Sutton *et al.*[17]. Note that we have neglected the Coulombic interactions from the excess charge, and the interaction of the net charges with the field from the plates: these turn out to be small effects.

Because the dimer shares its electron chemical potential with the two plates, its value, and hence N, depends on the bias. There will be net charge at non-zero bias, as can be seen from the following argument. For the empirical TB model used here, the atom is assigned a core charge of 0.48608. This leads to partial filling of the dimer bonding orbital, which in turn means the bonding orbital is pinned to the reference chemical potential (an analysis of the DOS can be found in section IV C). The pinning of the orbital requires the injection of slightly too many electrons into the dimer, producing a negative overall charge on the dimer atoms.

The equilibrium bond length $r = z$ corresponds to zero derivative of the energy with respect to bond length. This leads to the following dependence of the bond length on bias:

$$\frac{\Delta z}{z_0} = \left(\frac{N(0)}{N(V)}\right)^{1/(p-q)} - 1 \tag{12}$$

where z_0 is the equilibrium bond length at zero bias, and $\Delta z = z(V) - z_0$. The results of this model are compared with the results from the simulation in Fig. 6a, and excellent agreement is seen. Note that the variation with bias is nearly quadratic, as seen by the fitted trend line.

We now determine the polarizability α_E of the dimer from the variation of the charge difference between the two atoms with bias. In a linear approximation we have:

$$\Delta Q = \frac{2\alpha_E V}{z_0 d} \tag{13}$$

where ΔQ is defined as $Q_{\text{left}} - Q_{\text{right}}$, where Q_{left} is the charge on the left atom, and Q_{right} is the charge on the right atom. As the field direction is right to left, one would expect ΔQ to be positive, which is indeed in agreement with the behavior seen in Fig. 6b. However, the variation is clearly non-linear, which might be a consequence of the net charge of the dimer: this charge leads to an energy penalty when more electron density is added to one of the atoms.

As the dependence of Q on V is non-linear, we choose the initial gradient $\left.\frac{\mathrm{d}Q}{\mathrm{d}V}\right|_{V=0}$ of the quadratic fitted to the data to estimate the polarizability. The separation d between the two plates is 14.388 Å and z_0 is 2.15005 Å, yielding an initial polarizability of 37.03 a.u. (Note that 1 a.u. corresponds to 1.648777×10^{-41} C m^2 V^{-1}). Experimental polarizability values only exist for neutral copper atoms, so we can only compare the order of magnitude of the determined α_E to atomic values[18–22]. Calculated values range from 40.7 a.u. to 58.7 a.u., with 58.6 ± 4.7 a.u. being the experimental value[18]. The smaller value for the dimer relative to the free atom could well be a result of the minimal basis set used, which prevents polarization of individual atoms. However, the order of magnitude is the same.

There is one important consequence of the net charge on the dimer we have not yet considered. After relaxation, the dimer is only in a metastable state. If relaxed for long enough, it would eventually be pulled towards the positively charged plate. This was indeed what we observed upon increasing the number of relaxation steps.

C. Density of States

As previously mentioned, due to the empirical TB parametrization[17] used, the bonding orbital of the dimer is pinned to the reference chemical potential, which leads to high sensitivity of the number of electrons within the dimer to the bias, and results in a net negative charge of the dimer in all of our simulations. The density of states plot in Fig. 7 shows that the dimer's bonding orbital is indeed pinned to the reference electrochemical potential, and is approximately half filled. One can also see the expected relative shift in density of states of the right and the left capacitor plate produced by the applied bias.

D. Molecular Dynamics with Hairy Probes

We conclude by considering two sets of molecular dynamics simulations. In the first we take the system with

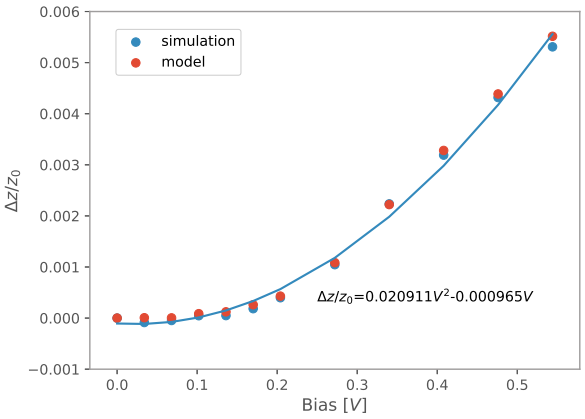

(a)

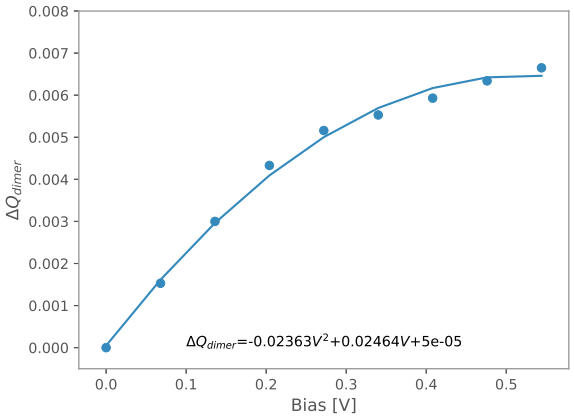

(b)

FIG. 6: a) The fractional change in bond length as a function of bias. The blue dots are from the simulation, the red dots are from our simple model, and the line is a quadratic fit. b) The charge difference between the dimer atoms as a function of bias; note that the behavior is not linear.

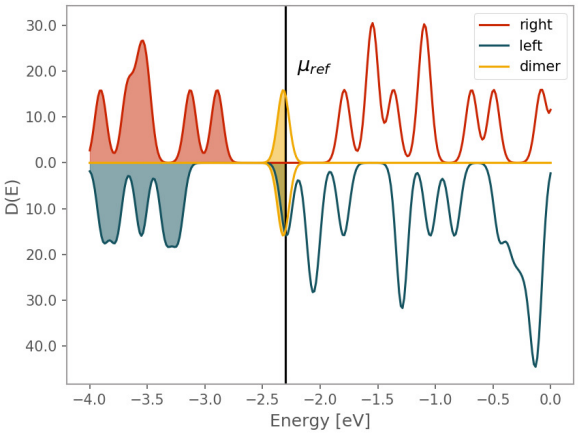

FIG. 7: The density of states for the setup shown in Fig. 1b after relaxation of the atomic forces. The upper (red) plot is the DOS projected onto all the atoms on the right plate, while the lower (grey) plot is the DOS projected onto all the atoms on the left plate. The dimer state is shown in yellow. The solution probe coupling strength is $\alpha = 0.01$, and the applied bias is 0.408 V. To make the plot smoother, we have applied a gaussian smearing of 0.05 eV.

the relaxed dimer with an applied bias of 0.408 V. For the second simulation we include a relaxed atomic wire that stretches between the two plates, linking them electronically. This simulation is intended to test the effect of the weak electronic coupling that could exist through a solution between electrodes. Our two main concerns are to see how the energy depends on time, as this is a good indicator of how close our atomic forces are to derivatives of the anzatz for the energy with respect to atomic displacement, and whether sensible results are still obtained once the plates are coupled. The mobile atoms are the Cu atoms in the two planes in each plate facing the other plate, plus the dimer or wire that sits between the plates.

For the dimer simulation, the total energy evolution of the system over time is shown in Fig. 8. We used a time step of 1 fs and an initial atomic temperature of 300 K. Note that the atoms to which the main probes have been attached (but not the solution probes) are not allowed to move. The fluctuations in energy shown in Fig. 8 are on the order of 0.001 Ry, with no systematic drift. This shows that the limiting case of Hairy Probes provides forces that are close enough to derivatives of the energy anzatz for us to perform MD simulations with open boundaries. This simple example simulation can be performed on a PC within a few hours, which opens the possibility of simulating larger electrochemical systems within a reasonable time frame.

For the simulation of the wire between the electrodes, we first relaxed the atoms in the wire, keeping the atoms in the plates at fixed positions, to remove large stresses. We then assigned random velocities corresponding to a temperature of 300 K to the atoms in the wire, and the two layers of atoms in each plate closest to the opposing plate. MD was performed under three sets of conditions: no probes attached (levels populated using a single Fermi-Dirac distribution with $k_BT = 0.136$ eV); probes attached, but with a bias of 0 V; probes attached and a bias of 0.136 V applied. The first two simulations are equivalent, except that no electron entropy is included in the energy when probes are attached.

In Fig. 9 we see how the energy varies with time for these simulations. We note the following points. First, there is a constant offset between the calculations with and without probes; this is due to the electron entropy term that is present in the absence of probes, but is absent otherwise. Second, the ripples in the energy when

the bias is applied are an order of magnitude bigger than for the other cases; their origin is still unclear. In addition, there are occasional spikes in the energy when the bias is applied; this is a result of full self-consistency not being achieved in the number of loops allowed, and reflects the increased difficulty of converging the charges. This might be because the energy is no longer variational, which would also explain the larger energy fluctuations under bias. Note that the wire breaks part way through the simulations; the wire atoms then gather on the surfaces of the plates.

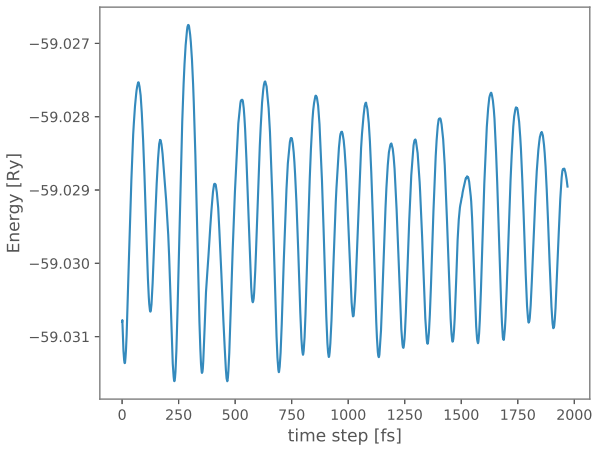

FIG. 8: The variation of energy trace with time from the molecular dynamics simulation of the system shown in Fig. 1b. The solution probe coupling strength is $\alpha = 0.01$, the bias is 0.408 V, and the initial temperature of the atoms is 300 K.

V. CONCLUSIONS

Here we have presented a simple open boundary scheme for electrons that is appropriate for electrochemical simulations in which any electric current is the result of the diffusion and drift of charged ions in solution. We note that we have not introduced a solution at this stage, but have considered various features that we find important by means of a simple model constructed from Cu atoms. The two plates approximate electrodes, the introduction of a dimer approximates a solvent or solute molecule in the field between the electrodes, and the wire approximates the weak electron coupling through the solution between the electrodes. These are only approximations, and key features are missing (notably the double layer and surface reactions), and these will be addressed in future work. Our scheme is derived as the limit of the Hairy Probes formalism in which the coupling of the probes to the system is weak. We note that the method evolves seamlessly to the full electron transport scenario if needed. By means of a simple TB model of a capacitor between whose plates a dimer and an atomic wire have been placed (the simplest approximations to an electrochemical cell we could envisage), we have shown that the forces are accurate enough, and the method efficient enough, that MD can be performed this way. This opens up a route to performing electronic structure simulations of non-equilibrium electrochemical processes at the atomic scale.

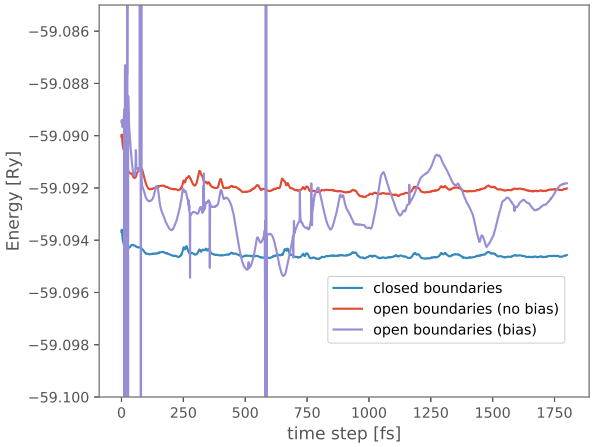

FIG. 9: The variation of energy trace with time from the molecular dynamics simulation of the system shown in Fig. 1c. The solution probe coupling strength is $\alpha = 0.01$, and the initial temperature of the atoms is 300 K. The blue line is from a calculation with no probes; the red line is from a system with probes but zero applied bias; the purple line is from a system with probes and a bias of 0.136 V applied.

ACKNOWLEDGMENTS

MGZ gratefully acknowledges funding from the EPSRC (EP/L015579/1) received through the Centre for Doctoral Training in the Theory and Simulation of Materials. APH acknowledges support from the Thomas Young Centre under grant TYC-10, and from the Leverhulme Trust under grant RPG-2014-125. Finally, we would like to thank the referees for many useful suggestions that have greatly improved this paper.

* mario.zauchner15@imperial.ac.uk
† a.horsfield@imperial.ac.uk
‡ t.todorov@qub.ac.uk

[1] J. O. Bockris and A. K. N. Reddy, *Modern Electrochemistry 2* (Plenum Press, 1973).
[2] J. Rossmeisl, E. Skúlason, M. E. Björketun, V. Tripkovic, and J. K. Nørskov, Chemical Physics Letters **466**, 68 (2008).
[3] C. Drechsel-Grau and M. Sprik, Molecular Physics **113**, 2463 (2015).
[4] M. Brandbyge, J.-L. Mozos, P. Ordejón, J. Taylor, and K. Stokbro, Phys. Rev. B **65**, 165401 (2002).
[5] A. R. Rocha and S. Sanvito, Phys. Rev. B **70**, 094406 (2004).
[6] T. Ozaki, K. Nishio, and H. Kino, Phys. Rev. B **81**, 035116 (2010).
[7] QuantumWise, "Atomistix toolkit, quantumwise a/s," (2015).
[8] A. P. Horsfield, M. Boleininger, R. D'Agosta, V. Iyer, A. Thong, T. N. Todorov, and C. White, Phys. Rev. B **94**, 075118 (2016), arXiv:1608.02789 [cond-mat.mes-hall].
[9] E. J. McEniry, D. R. Bowler, D. Dundas, A. P. Horsfield, C. G. Sánchez, and T. N. Todorov, Journal of Physics: Condensed Matter **19**, 196201 (2007).
[10] N. Bonnet, T. Morishita, O. Sugino, and M. Otani, Physical Review Letters **109**, 266101 (2012).
[11] A. P. Horsfield, Physical Review B **56**, 6594 (1997).
[12] S. Kenny and A. Horsfield, Computer Physics Communications **180**, 2616 (2009), 40 {YEARS} {OF} CPC: A celebratory issue focused on quality software for high performance, grid and novel computing architectures.
[13] A. P. Horsfield, D. Bowler, A. Fisher, T. N. Todorov, and C. G. Sánchez, Journal of Physics: Condensed Matter **16**, 8251 (2004).
[14] S. Datta, *Electronic transport in mesoscopic systems* (Cambridge university press, 1997).
[15] T. N. Todorov, G. A. D. Briggs, and A. P. Sutton, Journal of Physics: Condensed Matter **5**, 2389 (1993).
[16] A. P. Horsfield and A. M. Bratkovsky, Phys. Rev. B **53**, 15381 (1996).
[17] A. P. Sutton, T. N. Todorov, M. J. Cawkwell, and J. Hoekstra, Philosophical Magazine A **81**, 1833 (2001), http://dx.doi.org/10.1080/01418610108216639.
[18] L. Ma, J. Indergaard, B. Zhang, I. Larkin, R. Moro, and W. A. de Heer, Phys. Rev. A **91**, 010501 (2015).
[19] R. Pou-Amérigo, M. Merchán, I. Nebot-Gil, P.-O. Widmark, and B. O. Roos, Theoretica chimica acta **92**, 149 (1995).
[20] P. Neogrady, V. Kellö, M. Urban, and A. J. Sadlej, International Journal of Quantum Chemistry **63**, 557 (1997).
[21] B. O. Roos, R. Lindh, P.-A. Malmqvist, V. Veryazov, and P.-O. Widmark, The Journal of Physical Chemistry A **109**, 6575 (2005), pMID: 16834004, http://dx.doi.org/10.1021/jp0581126.
[22] P. Schwerdtfeger and G. A. Bowmaker, The Journal of Chemical Physics **100**, 4487 (1994), http://dx.doi.org/10.1063/1.466280.